contrast but is crystal-structure dependent when the eye is used to determine changes in image contrast. Thus, quantification of image intensities should be used for accurate composition determination by ARM. Lastly, although this study only considers systems containing two elements, the results indicate that similar principles can be used to interpret the contrast in systems containing combinations of three or more elements.

The authors are grateful to Dr M. A. O'Keefe for a critical review of this manuscript and to Dr J. Rose for several helpful discussions. This research was partially supported (JMH) by the National Science Foundation under Contract No. DMR-8657215. The authors also acknowledge N. Monda and Carnegie Mellon University for providing the computer funding.

References

ALLPRESS, J. G. & SANDERS, J. V. (1973). *J. Appl. Phys.* **6**, 165-190.
BURSILL, L. A. & SHEN, G. J. (1984). *Optik (Stuttgart)*, **66**, 251-276.
BURSILL, L. A., SHEN, G. J., SMITH, D. J. & BLANCHIN, M. G. (1984). *Ultramicroscopy*, **13**, 191-204.
COWLEY, J. M. (1973). *Acta Cryst.* A**29**, 529-540.
COWLEY, J. M. (1975). *Diffraction Physics*, pp. 283-292. Amsterdam: North-Holland.
COWLEY, J. M. & MOODIE, A. F. (1957). *Acta Cryst.* **10**, 609-619.
COWLEY, J. M. & MOODIE, A. F. (1958). *Proc. Phys. Soc.* **70**, 533-552.
DEDERICHS, P. H. (1973). *J. Phys. F*, **3**, 471-496.
GIBSON, J. M., MCDONALD, M. L., BATSTONE, J. L. & PHILLIPS, J. M. (1987). *Ultramicroscopy*, **22**, 35-46.
GLAISHER, R. W. & SPARGO, A. E. C. (1983). *Inst. Phys. Conf. Ser.* No. 68, pp. 185-190.
GOODMAN, P. & MOODIE, A. F. (1974). *Acta Cryst.* A**30**, 280-290.
HIRSCH, P., HOWIE, A., NICHOLSON, R. B., PASHLEY, D. W. & WHELAN, J. (1977). *Electron Microscopy of Thin Crystals*, pp. 201-207. Malabar: R. E. Krieger.
HOWE, J. M., DAHMEN, U. & GRONSKY, R. (1987). *Philos. Mag.* A**56**, 31-61.
HOWIE, A. & BASINSKI, Z. S. (1969). *Philos. Mag.* **149**, 1039-1063.
IIJIMA, S. (1977). *Optik (Stuttgart)*, **48**, 193-208.
ISAACSON, M. S., LANGMORE, J., PARKER, N. W., KOPF, D. & UTLAUT, M. (1976). *Ultramicroscopy*, **1**, 359-376.
LYNCH, D. F. & O'KEEFE, M. A. (1972). *Acta Cryst.* A**28**, 536-548.
MOTT, N. F. (1930). *Proc. R. Soc. London Ser. A*, **127**, 658-672.
O'KEEFE, M. A. (1973). *Acta Cryst.* A**29**, 389-401.
O'KEEFE, M. A. & BUSECK, P. R. (1979). *Trans. Am. Crystallogr. Assoc.* **15**, 27-46.
OURMAZD, A. (1987). *Proc. 45th Annual Meeting EMSA*, pp. 332-333. San Francisco: San Francisco Press.
OURMAZD, A., RENTSCHLER, J. R. & TAYLOR, D. W. (1986). *Phys. Rev. Lett.* **57**, 3073-3076.
PONCE, F. A. & O'KEEFE, M. A. (1986). *Proc. 44th Annual Meeting EMSA*, pp. 522-525. San Francisco: San Francisco Press.
REIMER, L. (1984). *Transmission Electron Microscopy, Principles of Image Formation and Microanalysis*, pp. 185-222. Berlin: Springer-Verlag.
ROSE, J. (1985). PhD Thesis. Univ. of California, Berkeley, USA.
ROSE, J. & GRONSKY, R. (1986). *Materials Problem Solving with the Transmission Electron Microscope*, pp. 57-64. Pittsburgh: MRS.
SAXTON, W. O. & SMITH, D. J. (1985). *Ultramicroscopy*, **18**, 39-48.
SCHERZER, O. (1949). *J. Appl. Phys.* **20**, 20-29.
SELF, P. G., GLAISHER, R. W. & SPARGO, A. E. C. (1985). *Ultramicroscopy*, **18**, 49-62.
SELF, P. G., O'KEEFE, M. A., BUSECK, P. R. & SPARGO, A. E. C. (1983). *Ultramicroscopy*, **11**, 35-52.
SMITH, D. J., SAXTON, W. O., O'KEEFE, M. A., WOOD, G. J. & STOBBS, W. M. (1983). *Ultramicroscopy*, **11**, 263-282.
SPENCE, J. C. H. (1981). *Experimental High-Resolution Electron Microscopy*, pp. 72-88. Oxford: Clarendon.
SPENCE, J. C. H., O'KEEFE, M. A. & IIJIMA, S. (1978). *Philos. Mag.* A**38**, 463-482.
TANAKA, N. & COWLEY, J. M. (1987). *Acta Cryst.* A**43**, 337-346.
VAN DYCK, D., VAN TENDELOO, G. & AMELINCKX, S. (1982). *Ultramicroscopy*, **10**, 263-280.

Acta Cryst. (1988). A**44**, 461-467

On the Treatment of Primary Extinction in Diffraction Theories Based on Intensity Coupling

BY JOCHEN R. SCHNEIDER, ODAIR D. GONÇALVES* AND HANS A. GRAF

Hahn-Meitner-Institut, Glienicker Strasse 100, *D*-1000 *Berlin* 39, *Federal Republic of Germany*

(*Received* 12 *June* 1987; *accepted* 11 *February* 1988)

Dedicated to Ulrich Bonse on the occasion of his 60th birthday

Abstract

Czochralski-grown silicon crystals of approximately 10 cm diameter and 1 cm thickness have been annealed at 1470 K in order to create a homogeneous defect structure, which is a basic condition for all statistical treatments of extinction. Absolute values of the integrated reflecting power of the 220, 440 and 660 reflections have been measured with 0·0392 Å γ-radiation in symmetrical Laue geometry for sample thicknesses between 1 and 3 cm. The amount of extinction in the experimental data varies between $y \simeq 0{\cdot}95$ and $y \simeq 0{\cdot}05$. Darwin's extinction theory has been used to describe the thickness dependence of the data sets. Despite some shortcomings of the model, it is shown that the assumption of a physically

* On leave from Instituto de Fisica, Universidade Federal do Rio de Janeiro, 21910 Rio de Janeiro RJ, Brazil.

0108-7673/88/040461-07$03.00

unrealistic Lorentzian mosaic distribution models the effect of primary extinction in an extinction theory based on the energy-transfer model. The sharp central part of the Lorentzian distribution produces a reduction of the effective sample thickness due to primary extinction, whereas the wings of the distribution dominate the correction for secondary extinction in the remaining part of the sample. A more flexible mosaic distribution function is proposed, which should be useful in cases of severe extinction.

Introduction

Today in most accurate structure refinements, the effect of extinction is corrected on the basis of an energy-transfer model presented by Zachariasen (1967) and Becker & Coppens (1974). The imperfections in the crystal are described within Darwin's mosaic model using parameters for the average size of the perfect blocks, and the standard deviation of a Gaussian or a Lorentzian mosaic distribution which describes their angular misorientation. This approach has some basic limitations as discussed by Kato (1976, 1979, 1980*a*), who more recently developed a statistical dynamical diffraction theory (Kato, 1980*b*) which, in principle, covers the full range from dynamical to kinematical diffraction behaviour as a function of two correlation parameters τ and E, the first describing short-range and the second long-range correlation. The relative merits of the two approaches to the extinction problem have been discussed by Becker & Dunstetter (1984).

People have been puzzled by the fact that the assumption of a Lorentzian mosaic distribution within the conventional energy-transfer coupling model often leads to a better agreement between measured and calculated structure factors, although a Gaussian is the more likely distribution, except for crystals showing deep surface damage due to grinding (Boehm, Prager & Barnea, 1974). Only a few attempts have been made in the past to develop an extinction correction for samples with inhomogeneous defect structure (*e.g.* Mazzone, 1981), an aspect which will not be treated in the present paper either. In general, the full width at half maximum (FWHM) of the Lorentzian distributions as determined from the structure refinements is unrealistically small.

In the present paper we want to demonstrate that the assumption of a Lorentzian mosaic distribution in the frame of an extinction theory based on intensity coupling only simulates the effect of primary extinction which, in principle, is due to the coupling of wave amplitudes in the perfect mosaic blocks. The argument is based on Darwin's extinction theory which proved to be successful in the interpretation of the integrated reflecting power measured with γ-radiation of wavelengths between 0·02 and 0·04 Å (Schneider & Kretschmer, 1985; Schneider, Jørgensen & Shirane, 1986). The samples are annealed Czochralski-grown silicon crystals which are characterized by double-crystal γ-ray rocking curves measured with 1·4″ arc resolution, as well as by high-resolution X-ray topography and double-crystal X-ray rocking curves measured with 0·25″ arc resolution (Schneider, Gonçalves, Rollason, Bonse, Lauer & Zulehner, 1988). The crystals show highly homogeneous defect structure. Using 0·0392 Å γ-radiation, we measured the integrated reflecting power on an absolute scale for various sample thicknesses achieved by tilting the large disc-shaped crystals around the scattering vector. The thickness dependence of the measured integrated reflecting power was fitted by Darwin's extinction theory assuming a Gaussian or Lorentzian mosaic distribution, respectively, and by introducing an effective thickness, $T_{\rm eff}$, smaller than the geometrical thickness, T_0, in order to parametrize primary extinction.

Darwin's extinction theory

According to De Marco & Weiss (1965), the integrated reflecting power for diffraction of γ-rays in Laue geometry through a plane-parallel perfect single crystal is given by

$$R_H^{\rm dyn} = \frac{r_0 |F'_H| e^{-W} \lambda^2}{\pi V_{\rm cell} (|b|)^{1/2} \sin 2\theta_B} R_{\rm H}^{\gamma,\rm dyn}({\rm Laue}) \quad (1)$$

where r_0 is the classical electron radius, F'_H is the real part of the structure factor, e^{-W} the Debye-Waller factor, and $V_{\rm cell}$ the volume of the unit cell. λ represents the wavelength, and θ_B is the Bragg angle. b represents the ratio of the direction cosines γ_0 and γ_H and is equal to unity for symmetrical Laue geometry. For diffraction experiments with γ-radiation of wavelength of the order of 0·04 Å on silicon crystals, $R_H^{\gamma,\rm dyn}$(Laue) is well approximated by

$$R_H^{\gamma,\rm dyn}({\rm Laue}) = \tfrac{1}{2}\pi \exp(-\mu_0 t/\cos\theta_B) \int_0^{2A} J_0(x)\,{\rm d}x \quad (2)$$

with

$$A = \frac{r_0 |F'_H| e^{-W} \lambda t}{V_{\rm cell} (|\gamma_0 \gamma_H|)^{1/2}} = \frac{t}{t_{\rm ext}}. \quad (3)$$

$\mu_0 = 0{\cdot}25$ cm^{-1} is the linear attenuation coefficient measured with 0·0392 Å γ-radiation in silicon, and t represents the thickness of the crystal plate. $J_0(x)$ is the zeroth-order Bessel function of the first kind. The justification of the approximations involved in deriving (2) was discussed by Graf & Schneider (1986). The thickness t corresponding to $A = 1$ is defined as the extinction length, $t_{\rm ext}$, which is inversely proportional to the structure factor and the wavelength. Thus the parameter A is a measure of the sample thickness in units of the extinction length.

In Fig. 1 the dynamical integrated reflecting power $R_H^{y,\mathrm{dyn}}$(Laue) is plotted as a function of the parameter A together with the integrated reflecting power

$$R_H^{y,\mathrm{kin}}(\mathrm{Laue}) = \pi A \tag{4}$$

calculated from kinematical theory for an ideally imperfect single crystal.

$$\begin{aligned} R_H^{\mathrm{kin}} &= \frac{r_0|F'_H|e^{-W}\lambda^2}{\pi V_{\mathrm{cell}}(|b|)^{1/2}\sin 2\theta_B} R_H^{y,\mathrm{kin}}(\mathrm{Laue}) \\ &= r_0^2 \frac{|F'_H|^2 e^{-2W}}{V_{\mathrm{cell}}^2} \frac{\lambda^3}{\sin 2\theta_B} \frac{t}{\cos\theta_B} \\ &= Qt/\cos\theta_B. \end{aligned} \tag{5}$$

Because of the small Bragg angles, the polarization factor is well approximated by unity. For sample thicknesses $t \le t_{\mathrm{ext}}/2$, both theories provide identical values for the integrated reflecting power and therefore only for samples of thickness smaller than half an extinction length is it guaranteed that the diffraction is free of extinction. Structure factors have been measured with synchrotron radiation of $\lambda = 0{\cdot}91$ Å on a 6 μm CaF_2 single crystal (Bachmann, Kohler, Schulz & Weber, 1985). Compared with a 90 μm sample, extinction was very much reduced for the smaller crystal, which indicates that extinction-free diffraction may be obtained for such tiny crystals. On the other hand, even on larger crystals extinction can be excluded by working with shorter-wavelength radiation. In the case of silicon 220, one finds $t_{\mathrm{ext}}/2 \simeq 4{\cdot}5$ μm for $\lambda = 0{\cdot}91$ Å and ≃100 μm for $\lambda = 0{\cdot}0392$ Å. For the extinction correction, it is not the absolute size of the sample which is of importance, but its relation to the extinction length which depends on wavelength and structure factor.

If the thickness of the perfect blocks in a mosaic crystal is larger than about one extinction length, part of the block does not contribute to an increase of the scattered intensity as expected from kinematical theory, where the scattering power is proportional to the number of atoms in the crystal. This reduction of the integrated reflecting power of a mosaic block with respect to R_H^{kin} is called primary extinction and can be visualized in an 'absorbing hole' model (Schneider, 1977). Compared with the geometrical thickness T_0 of the mosaic crystal primary extinction leads to a reduction of the sample thickness to be used in the expression for the calculation of the integrated reflecting power.

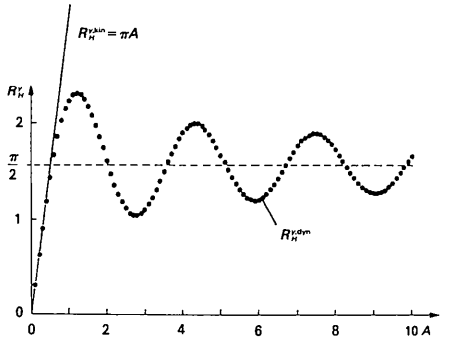

Fig. 1. Integrated reflecting power for symmetrical Laue geometry calculated from dynamical and kinematical diffraction theory for zero absorption as a function of the parameter A, which is a measure of the sample thickness in units of the extinction length. Because of the small Bragg angles for the diffraction of 0·0392 Å γ-radiation at low-order reflections, the polarization factor is very close to unity, and no fading of the *Pendellösung* oscillations can be observed.

Darwin's extinction theory starts from the intensity transfer equations (Laue geometry)

$$\begin{aligned} \mathrm{d}P_0/\mathrm{d}T &= -\mu_0 P_0 - \sigma P_0 + \sigma P_H \\ \mathrm{d}P_H/\mathrm{d}T &= -\mu_0 P_0 + \sigma P_0 - \sigma P_H \end{aligned} \tag{6}$$

$P_0(T)$ and $P_H(T)$ represent the power of the incident and diffracted beams, respectively, at a depth T, and μ_0 is the total linear attenuation coefficient. In symmetrical Laue geometry, the length of the transmitted and the diffracted beam path is equal to $T_0/\cos\theta_B$. For the coupling constant σ one obtains

$$\sigma(\omega) = W(\omega) R_H^*/\bar{t} \tag{7}$$

where $\bar{t}$ is the mean block thickness and R_H^* represents the integrated reflecting power calculated from dynamical theory for a perfect plane-parallel plate of infinite lateral extension and thickness $\bar{t}$. $W(\omega)$ is the mosaic distribution function. If $t \le t_{\mathrm{ext}}/2$, there is no primary extinction, $R_H^* = R_H^{\mathrm{kin}}$, and using the quantity Q defined in (5) one obtains

$$\sigma(\omega) = W(\omega) Q/\cos\theta_B. \tag{8}$$

The solution of Darwin's intensity transport equations leads to the following expression for the theoretical reflectivity distribution:

$$\begin{aligned} r_{\mathrm{th}}(\omega) &= P_H(\omega)/[P_0 \exp(-\mu_0 T_0/\cos\theta_B)] \\ &= \tfrac{1}{2}\{1 - \exp[-2\sigma(\omega) T_0]\}. \end{aligned} \tag{9}$$

Kinematical diffraction theory assumes that $\mathrm{d}P_H = \sigma P_0 \mathrm{d}T$ ($\mu_0 = 0$), *i.e.* the attenuation of the incident beam due to diffraction as well as the possibility of multiple scattering is neglected. Equation (6) takes both effects into account, and the calculated reflectivity will be smaller than the kinematical value, which is visualized by expanding the exponential in (9) to second order:

$$r_{\mathrm{th}}(\omega) \simeq R_H^{\mathrm{kin}} W(\omega)[1 - R_H^{\mathrm{kin}} W(\omega)]. \tag{10}$$

This reduction of the integrated reflecting power of a real crystal with respect to R_H^{kin} is called secondary extinction. The kinematical limit is reached only if $R_H^{\mathrm{kin}} W(\omega) \ll 1$ over the whole scan range. If primary extinction cannot be excluded, the geometrical sample thickness T_0 in (9) should be replaced by an

effective thickness $T_{\rm eff} < T_0$, which has to be determined together with the full width at half maximum (FWHM) of a Gaussian or Lorentzian mosaic distribution by fitting the model to appropriate experimental data.

γ-ray diffractometry

Absolute values of the integrated reflecting power were measured in symmetrical Laue geometry using 0·0392 Å γ-radiation from ^{192}Ir (Schneider, 1983). The beam cross section was 2 × 4 mm, and the angular divergence is approximately 3·2′ arc in the scattering and 6·4′ in the vertical plane. In a double-crystal set-up (Schneider & Graf, 1986), the direct γ-ray beam is further collimated to an angular divergence of 1·4″ arc by diffraction from an internally strained silicon crystal. After subtraction of the linear background, P_B, the reflected intensity is normalized with the transmitted intensity measured in an angular range where no Bragg diffraction occurs. The reflectivity distribution so defined,

$$r(\omega) = \frac{P_H(\omega) - P_B}{P_0 \exp\left[-\mu_0 T_0 / \cos\theta_B\right]}. \qquad (11)$$

can be directly compared with the theoretical reflectivity $r_{\rm th}(\omega)$ from (9), provided there is no deconvolution problem. The samples are mounted in a large Huber χ-φ circle with the scattering vector parallel to the φ axis so that the thickness of the sample can be varied by changing φ. In order to test extinction theories by means of γ-ray diffractometry, large samples with a homogeneous defect structure are needed, and it turned out that annealed Czochralski-grown silicon crystals are well suited for such studies.

Annealed silicon single crystals

Disc-shaped single crystals of approximately 1 cm thickness have been cut from Czochralski-grown crystals of 10 cm diameter produced by Wacker-Chemitronic, Burghausen, Federal Republic of Germany. All samples have been polished chemically. The growth direction was [001], the resistivity of the boron-doped crystals is 90 Ωcm, they contain $7{\cdot}7 \times 10^{17}$ cm^{-3} oxygen atoms on interstitial and $0{\cdot}2 \times 10^{17}$ cm^{-3} carbon atoms on substitutional sites. Sample CZ 286.788/127/1T (in the following CZ-1T for short) was annealed for 8 h at 1470 K, sample 286.788/127/2T (in the following CZ-2T) was first annealed for 2 h at 1020 K and subsequently for 8 h at 1470 K.

During crystal growth the silica crucible partly dissolves into the silicon melt, and, subsequently, relatively large quantities of oxygen are incorporated into the growing crystal. In the dissolved state, these oxygen atoms occupy distorted bond-centred positions. At temperatures above 820 K, oxygen forms precipitates as some form of silica. For annealing in the temperature range from approximately 920 to 1050 K, the dominant precipitate morphology is rod-like (Tempelhoff, Gleichmann, Spiegelberg & Wruch, 1979) and has been identified as coesite, a high-pressure form of quartz (Bourret, Thibault-Dessaux & Seidmann, 1984; Ponce & Hahn, 1984). The silicon matrix around the evenly distributed precipitates is strained. At temperatures higher than 1170 K the strain around the growing SiO_2 precipitates can be released by plastic deformation which condenses to stacking faults, the edges of which are partial dislocation loops. Therefore annealed Czochralski-grown silicon crystals are well suited for extinction studies.

The samples have been characterized by γ-ray diffractometry, as well as by high-resolution X-ray topography (Schneider *et al.*, 1988). Fig. 2 shows a double-crystal rocking curve measured with 0·0392 Å γ-radiation and an angular resolution of 1·4″ arc. After deconvolution its FWHM is of the order of 2″ arc, and the shape can be well approximated by a Gaussian.

Integrated reflecting power *versus* sample thickness

The integrated reflecting power was measured with 0·0392 Å γ-radiation in both annealed silicon crystals at reflections 220, 440 and 660 for sample thicknesses varying between 1 and 3 cm. For each sample thickness the kinematical integrated reflecting power was calculated, and in Fig. 3 the extinction coefficient $y^{\rm obs}(T_i) = R_H^{\rm obs}(T_i)/R_H^{\rm kin}(T_i)$ is plotted as a function of T_i. The amount of extinction varies between $y \simeq 0{\cdot}05$ and $y \simeq 0{\cdot}95$. The data from sample CZ-1T, annealed for 8 h at 1470 K, are more strongly affected by extinction than those from sample CZ-2T subject to a two-step anneal, *i.e.* 2 h at 1020 K and then 8 h at 1470 K.

With a Gaussian or Lorentzian mosaic distribution, the integrated reflecting power $R_H^{\rm theor}(T_i)$ was calculated by integrating (9) for $1 \le T_i \le 3$ cm. In order to

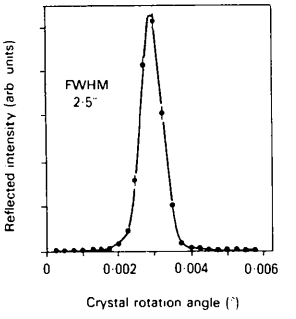

Fig. 2. Double-crystal γ-ray rocking curve measured with 1·4″ arc angular resolution at the 220 reflection of sample CZ-2T for zero tilt angle, *i.e.* the [001] growth direction is in the scattering plane. Sample thickness $T_0 = 1$ cm, wavelength $\lambda = 0{\cdot}0392$ Å, cross section of the incident beam 2 × 4 mm.

determine the FWHM of the mosaic distribution as well as the ratio $T_{\rm eff}/T_0$, the theoretical extinction factor $y^{\rm theor}(T_i)=R_H^{\rm theor}(T_i)/R_H^{\rm kin}(T_i)$ was implemented as a subroutine in the standard fit program *MINUIT* (James & Ross, 1975). The function minimized by this program is

$$\chi^2=\sum_{i=1}^{N}\left|\frac{R_i^{\rm obs}-R_i^{\rm theor}}{\sigma_i^{\rm obs}}\right|^2 \qquad (12)$$

where N is the number of observations, *i.e.* the number of different thicknesses T_i for which the integrated reflecting power $R_i^{\rm obs}$ was measured, and $\sigma_i^{\rm obs}$ is the standard deviation of $R_i^{\rm obs}$ essentially derived from counting statistics. The curves through the experimental data shown in Fig. 3 represent the best fit obtained for a Lorentzian mosaic distribution.

The extinction parameters obtained by fitting Darwin's extinction model with Gaussian or Lorentzian mosaic distributions to the six experimental data sets are summarized in Table 1. The quality of the fits is described as usual by the goodness of fit

$$\mathrm{GOF}=\chi^2/(N-p), \qquad (13)$$

with N the number of observations and p the number of parameters, and the agreement factor

$$R=100[\chi^2/\textstyle\sum_{i=1}(R_i^{\rm obs}/\sigma_i^{\rm obs})^2]^{1/2}. \qquad (14)$$

If we disregard for the moment the data sets showing the smallest and the largest amount of extinction, a Lorentzian mosaic distribution allows us to fit the data well without the necessity of introducing an effective sample thickness $T_{eff}<T_0$. On the other hand, the values of the FWHM of the mosaic distribution are of the order of 0·2″ arc, which is nearly one order of magnitude smaller than the FWHM of the measured rocking curves.

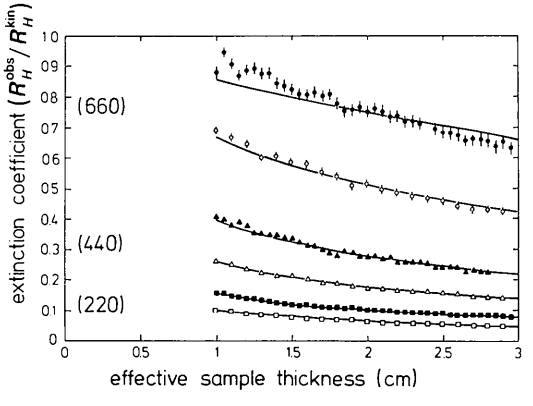

Fig. 3. Ratio of the measured integrated reflecting power and the corresponding value calculated from kinematical theory as a function of sample thickness. The solid points represent data from sample CZ-2T (annealed for 2 h at 1020 K and subsequently for 8 h at 1470 K), the open points data from sample CZ-1T (annealed for 8 h at 1470 K). The solid lines represent the best fit of Darwin's extinction model using a Lorentzian mosaic distribution. The experimental data are corrected for absorption and time decay of the γ-ray source. Cross section of the incident γ-ray beam 2×4 mm, wavelength $\lambda=0{\cdot}0392$ Å.

In addition, the shape of the measured rocking curves does not support the assumption of a Lorentzian mosaic distribution in the extinction model. With the more realistic Gaussian mosaic distribution, the fits to the experimental data are of similar quality, but now an effective thickness of $T_{\rm eff}<T_0$ has to be introduced, which indicates that the diffraction is affected by primary extinction. The FWHM of the mosaic distribution is of the order of 1″ arc and in better agreement with the experimental values.

From an initial Lorentzian mosaic distribution of FWHM = 0·266″ arc, the reflectivity distribution was calculated from (9) for silicon 220 and wavelengths between $\lambda=0{\cdot}0392$ Å, sample thickness $T_0=1$ cm. The results are shown in Fig. 4. In the case of $\lambda=0{\cdot}0039$ Å extinction is very small and $r_{\rm th}(\omega)$ is proportional to the mosaic distribution $W(\omega)$, which describes the probability of finding regions in the crystal with lattice plane orientations between ω and $\omega+{\rm d}\omega$. The reflectivity distribution is centred on the Bragg angle, $\omega_0=\theta_B$, and for negligible extinction the angular range $[\omega_0-\Gamma_L,\omega_0+\Gamma_L]$ represents 50% of the crystal volume, where Γ_L is the half-width at half maximum of the Lorentzian. More generally, a partition ratio can be defined as the ratio of the reflecting power integrated in the limits of $\omega=\omega_0-\Gamma_L$ and $\omega=\omega_0+\Gamma_L$, and the integral over the full reflectivity distribution. If the wavelength and thus the amount of secondary extinction is increased, the reflectivity distribution in its central region rapidly reaches the value of 0·5, which is the maximum value for a non-absorbing crystal in Laue geometry. As shown in the inset of Fig. 4, for $\lambda=0{\cdot}0392$ Å 50% of the crystal volume contributes only about 10% to the total integrated reflecting power, which corresponds to a reduction of the active volume to about 60% of the total. However, by fitting with a Gaussian mosaic distribution, the effective thickness was reduced to 0·275 T_0, *i.e.* twice as strong. This discrepancy is essentially due to the different normalizations of the two distributions. If Γ(Gaussian) = Γ(Lorentzian), the integral over the Lorentzian is about twice that over the Gaussian so that one obtains for the leading term in (10)

$$R_H^{\rm kin}(\mathrm{Lorentzian})\simeq 2R_H^{\rm kin}(\mathrm{Gaussian})|_{\Gamma_G=\Gamma_L}. \qquad (15)$$

In the limit of small extinction, both expressions have to approach identical values, which implies that the effective thickness of the crystal with Gaussian mosaicity is half the value of that with Lorentzian mosaic distribution of the same half-width.

Closer inspection of the data presented in Table 1 reveals a number of inconsistencies in the extinction model discussed so far. The thickness dependence of the 220 integrated reflecting power measured for

Table 1. *Values of the FWHM of the mosaic distribution ($\Delta\omega_M$) and the ratio of the effective to the geometrical sample thickness (T_{eff}/T_0) obtained from fitting Darwin's extinction theory to the thickness dependence of the integrated reflecting power measured with* 0·0392 Å *γ-radiation at reflections* 220, 440 *and* 660 (*see Fig.* 3)

Sample CZ-1T is a Czochralski-grown silicon crystal annealed for 8 h at 1470 K, CZ-2T was first annealed for 2 h at 1020 K and subsequently for 8 h at 1470 K. The agreement factor, R, and the goodness of fit, GOF, are defined in the text

	Reflection	660	660	440	440	220	220
	Sample	2T	1T	2T	1T	2T	1T
Darwin (Lorentz)	$\Delta\omega_M$(″)	0·563 (6)	0·185 (2)	0·317 (2)	0·139 (1)	0·266 (1)	0·147 (7)
	T_{eff}/T_0	1·0000 (4)	1·000 (2)	1·000 (6)	1·00 (2)	1·000 (6)	0·81 (7)
	R(%)	4·2	2·3	2·5	1·7	1·4	1·7
	GOF	7·3	2·9	2·9	1·7	1·4	1·5
Darwin (Gauss)	$\Delta\omega_M$(″)	1·20 (1)	0·465 (8)	1·28 (2)	0·81 (1)	2·16 (2)	1·37 (2)
	T_{eff}/T_0	1·0000 (4)	0·98 (2)	0·66 (1)	0·43 (1)	0·275 (4)	0·176 (5)
	R(%)	3·8	1·1	1·9	2·0	1·6	2·1
	GOF	5·9	0·7	1·7	2·4	1·9	2·3

sample CZ-1T cannot be described by reducing the FWHM of the Lorentzian distribution. Primary extinction is too strong, and the effective thickness has to be reduced even for this model. It is not clear why the data taken at the 660 reflection of sample CZ-2T, which is affected least of all by extinction, cannot be described by the present extinction model. For each sample the three data sets were measured in the same crystal volumes, and one expects that the FWHM of the mosaic distributions obtained from the fit should be identical. The calculated values, however, vary by about a factor of two, which reflects a shortcoming of the model. On the other hand, the observed reduction of the effective thickness with decreasing order of reflection is expected from the model, because the extinction length is inversely proportional to the structure factor.

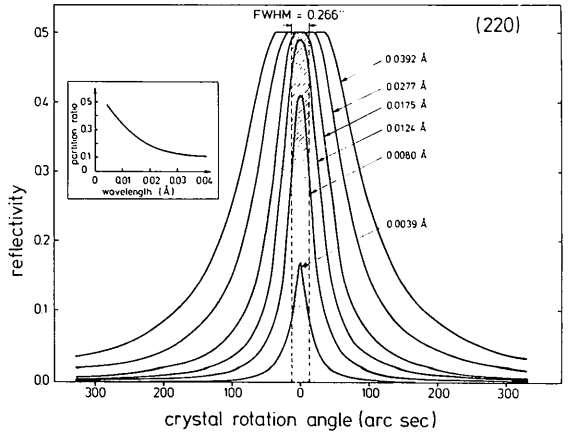

Fig. 4. Reflectivity distribution calculated from Darwin's expression for secondary extinction only [equation (9)] for silicon 220, sample thickness $T_0 = 1$ cm, and a Lorentzian mosaic distribution of FWHM = 0·266″. The wavelength is varied in the range from 0·0039 to 0·0392 Å, the wavelength of the γ-ray beam used to measure the data shown in Fig. 3. The partition ratio shown in the inset is defined as the ratio of the reflectivity $r_{th}(\omega)$ integrated in the limits of $(\omega_0 - \Gamma_L) \leq \omega \leq (\omega_0 + \Gamma_L)$ and the integral over the full reflectivity distribution. Γ_L is the half-width at half-height of the Lorentzian mosaic distribution.

Concluding remarks

Despite the shortcomings of the extinction model applied to interpret the thickness dependence of the integrated reflecting power measured with 0·0392 Å γ-radiation at the 220, 440 and 660 reflections of two annealed Czochralski-grown silicon crystals, it has been shown that the assumption of a Lorentzian mosaic distribution models the effect of primary extinction in an extinction theory based on the energy-transfer model. The sharp central part of the Lorentzian produces a reduction of the effective sample thickness due to primary extinction, whereas the wings of the distribution dominate the correction for secondary extinction in the remaining part of the sample, active in the energy-transfer model.

Fig. 5 shows that a Lorentzian distribution can be reasonably well reproduced by the sum of two Gaussians each normalized to 0·5, the Lorentzian being normalized to 1. Because there is no physical justification for assuming a Lorentzian mosaic distribution, its incorporation into the refinement corre-

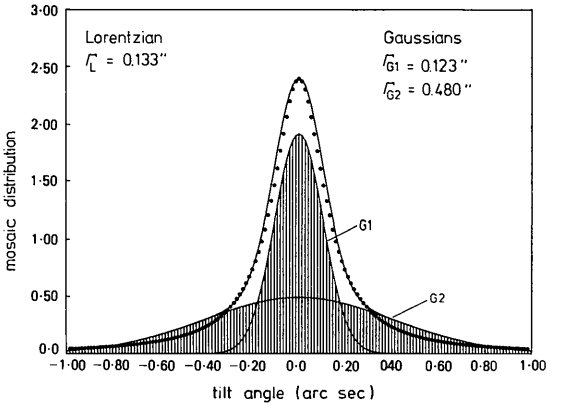

Fig. 5. Best fit of the superposition of two Gaussians normalized to 0·5 to a Lorentzian normalized to 1. The latter is represented by the dots. Γ_L and Γ_{G1}, Γ_{G2} are the half-widths at half-maximum of the Lorentzian and Gaussian distributions, respectively.

sponds to the introduction of a second parameter, both being correlated by a ratio of approximately 4:1.

Qualitatively, the narrow Gaussian models primary extinction and the four-times-wider Gaussian models secondary extinction. There is no physical reason for the constraint of the ratio of 4:1 for the half-widths of the two Gaussians as imposed by the assumption of a Lorentzian mosaic distribution. The model should become much more flexible if the ratio of the half-widths is a free parameter in some fixed limits. Additionally the relative normalization of the two Gaussians can be introduced as a free parameter under the natural constraint that the sum of the two must normalize to 1.

References

BACHMANN, R., KOHLER, H., SCHULZ, H. & WEBER, H.-P. (1985). *Acta Cryst.* A**41**, 35-40.

BECKER, P. J. & COPPENS, P. (1974). *Acta Cryst.* A**30**, 129-147, 148-153.

BECKER, P. & DUNSTETTER, F. (1984). *Acta Cryst.* A**40**, 241-251.

BOEHM, J. M., PRAGER, P. R. & BARNEA, Z. (1974). *Acta Cryst.* A**30**, 335-337.

BOURRET, A., THIBAULT-DESSAUX, J. & SEIDMANN, D. N. (1984). *J. Appl. Phys.* **55**, 825-836.

DEMARCO, J. J. & WEISS, R. J. (1965). *Acta Cryst.* **19**, 68-72.

GRAF, H. A. & SCHNEIDER, J. R. (1986). *Phys. Rev. B*, **34**, 8629-8638.

JAMES, F. & ROSS, M. (1975). *Comput. Phys. Commun.* **10**, 343-367.

KATO, N. (1976). *Acta Cryst.* A**32**, 453-457, 458-466.

KATO, N. (1979). *Acta Cryst.* A**35**, 9-16.

KATO, N. (1980*a*). *Acta Cryst.* A**36**, 171-177.

KATO, N. (1980*b*). *Acta Cryst.* A**36**, 763-769, 770-778.

MAZZONE, G. (1981). *Acta Cryst.* A**37**, 391-397.

PONCE, F. A. & HAHN, H. (1984). In *Electron Microscopy of Materials, Mater. Res. Soc. Proc.*, Vol. 31, edited by W. KRAKOW, D. A. SMITH & L. W. HOBBS, p. 153. New York: North Holland.

SCHNEIDER, J. R. (1977). *Acta Cryst.* A**33**, 235-243.

SCHNEIDER, J. R. (1983). *J. Cryst. Growth*, **65**, 660-671.

SCHNEIDER, J. R., GONÇALVES, O. D., ROLLASON, A. J., BONSE, U., LAUER, J. & ZULEHNER, W. (1988). *Nucl. Instrum. Methods Phys. Res.* B**29**, 661-674.

SCHNEIDER, J. R. & GRAF, H. A. (1986). *J. Cryst. Growth*, **74**, 191-202.

SCHNEIDER, J. R., JØRGENSEN, J. E. & SHIRANE, G. (1986). *Phase Transitions*, **8**, 17-34.

SCHNEIDER, J. R. & KRETSCHMER, H. R. (1985). *Z. Naturwiss.* **72**, 249-259.

TEMPELHOFF, K., GLEICHMANN, R., SPIEGELBERG, F. & WRUCH, D. (1979). *Phys. Status Solidi A*, **56**, 213-223.

ZACHARIASEN, W. H. (1967). *Acta Cryst.* **23**, 558-564.

Acta Cryst. (1988). A**44**, 467-478

Evaluating Finite Fourier Transforms that Respect Group Symmetries

BY L. AUSLANDER

Department of Mathematics, CUNY Graduate Center, 33 West 42 St, New York, NY 10036, USA

R. W. JOHNSON

Department of Computer Science, CUNY Graduate Center, 33 West 42 St, New York, NY 10036, USA

AND M. VULIS

Department of Computer Science, CCNY, Convent Ave at 138th St, New York, NY 10031, USA

(*Received* 28 *February* 1987; *accepted* 12 *February* 1988)

Abstract

A general method for producing efficient algorithms to evaluate finite Fourier transforms that fully utilize symmetry to reduce both computing time and space requirements is described. The method is applicable to all space groups. The resulting algorithms retain the '$N \log N$' behavior of the fast Fourier transform while reducing the size of the data to approximately an asymmetric unit. The algorithm for the $p3$ and $P3$ groups is shown.

0108-7673/88/040467-12$03.00

I. Introduction

The standard method for efficiently computing three-dimensional finite Fourier transforms is by Cooley-Tukey and Good-Thomas algorithms. Ten Eyck (1973) in his pioneering work on crystallographic fast Fourier transforms showed how certain groups of crystallographic symmetries could be combined with such algorithms to reduce the computational burden. There are two main features of the Ten Eyck algorithms: (1) the groups of symmetries must carry